

Point-Dipole Approximation of the Exciton Coupling Model Versus Type of Bonding and of Excitons in Porphyrin Supramolecular Structures

Josep M. Ribó,* Josep M. Bofill, Joaquim Crusats, and Raimon Rubires^[a]

Abstract: The application of the exciton coupling model to interacting porphyrin chromophores is discussed. Covalently bonded systems and ionic or electrostatically bonded homoassociates require different orientations of the transition dipole moments in order to explain the experimental results: according to the symmetry of the assembly for covalently bonded porphyrins, and assuming isolated chromophores for ionic bonded porphyrins. Further, for covalently bonded systems, an extended exciton coupling has been demonstrated, but the ionic systems are in agreement with non-extended couplings. The relation of these facts to a molecular description of solid-state Wannier–Mott or Frenkel excitons is briefly discussed.

Keywords: electronic structure • porphyrinoids • solid-state chemistry • UV/Vis spectroscopy

Introduction

A new emerging field for organic materials is the development of new nanodevices, through self-assembly towards supramolecular structures or synthesis of molecules of nanoscale and submicroscale size. For the design and supramolecular engineering of these materials it is necessary to have simple reliable models that relate the structural and electronic models used in organic chemistry with those used in chemical physics and solid-state physics and chemistry. Moreover, these predictions must be made for the borderline that separates the electronic description between orbital models (molecules and supramolecules) and band models (bulk condensed phase).

In solid-state chemistry, the quasi-particle exciton, generated by the mutual interaction and spatial correlation of an electron-hole pair, is used to explain many electronic properties of semiconductors and insulators.^[1]

The physical dimer of a chromophore shows an electronic absorption spectrum different from that of the isolated chromophore, owing to the interaction between the excited chromophore and the neighboring ground-state chromophore. This implies the interaction and spatial correlation of the electron-hole pair generated by the photon absorption and represents at a molecular level the excitons of an aggregated state of matter. The exciton coupling model in its simple exciton point-dipole form^[2] (Figure 1) is applied to

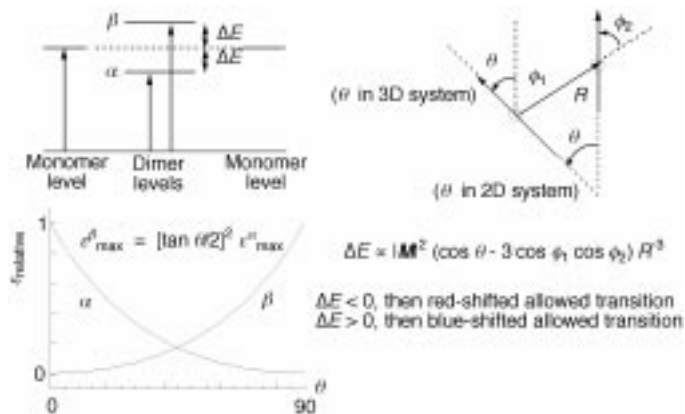


Figure 1. Point-dipole approximation of the exciton coupling model.^[1, 2] For the sign of the angles the sense of the distance vector (R) must be taken into account. The “direction” of the transition dipole moments is inferred from chemical reasoning (e.g., HOMO \rightarrow LUMO). In the case of symmetric substituted chromophores, like the porphyrins described here, the sense of the transition dipole is that resulting in the highest vector sum better aligned in the sense of “growth” of the system.

[a] Prof. Dr. J. M. Ribó, Prof. tit. Dr. J. M. Bofill, Dr. J. Crusats, Dr. R. Rubires
 Departament de Química Orgànica
 Universitat de Barcelona
 c/ Martí i Franquès 1, 08028-Barcelona (Spain)
 Fax: (+34) 93-3397878
 E-mail: jmr@qo.ub.es

relate the UV/Vis spectra of chromophore dimers and oligomers to their stereochemistry. This model is especially useful for chiral systems^[3], because it allows us to relate the circular dichroism (CD) spectra to the chirality sign of the arrangement between chromophores. More accurate models and approximations are not used by organic chemists, who

prefer user-friendly methods that provide fast qualitative predictions.

Here, we describe the application of the point-dipole approximation of the exciton coupling model and its relation to the solid-state type of excitons.

The application of the qualitative exciton coupling treatment (Figure 1) to chromophore J-aggregates (side-to-side) and H-aggregates (face-to-face),^[4] that is, for the two extreme cases of Figure 1 when the allowed state transition corresponds to the low- or to the high-energy state, respectively, give rise to bathochromic and hypsochromic shifts, respectively, in agreement with the experimental results. In the case of porphyrins and phthalocyanines it allows to distinguish between lateral and π stacking.^[5] This is commonly performed by the observation of the spectral shift shown by the B-band (Soret-band; $S_0 \rightarrow S_2$) of the tetrapyrrolic cyclic system, which generally shows higher oscillator strengths and, in consequence, higher shift values than the Q-bands ($S_0 \rightarrow S_1$). However, the application of this approximation to porphyrin and phthalocyanine supramolecular systems, in order to infer structural details, can lead to erroneous conclusions, because of the degeneration of the B-band (B_x and B_y). Therefore, the relative alignment of the two transitions in the individual chromophores of the dimer or oligomer must be taken into

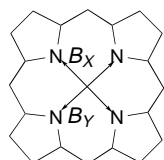


Figure 2. Orientation of the Soret band (B-band) according to Gouterman.^[6]

account. According to Gouterman's four-orbital porphyrin model,^[6] in the "monomeric" porphyrin both transition dipole moments are aligned with the opposite nitrogen atoms (Figure 2). In the published papers on tetrapyrrolic supramolecular systems, the relative alignments between the pairs of orthogonal transition dipole moments are normally defined

according to the highest possible symmetry given by the geometry of the system. However, although the point-dipole approximation is used to infer the structure,^[7] the lack of criteria to set the relative orientation between the pairs of transition dipole moments results in structure determinations of low significance.

Here we analyze two published cases, which are explained through the alignment of the transition dipole moments

according to: **a)** the highest possible symmetry of the pairs of transition dipole moments fitted to the geometry of the supramolecular assembly, or **b)** those of the individual chromophores (Gouterman's model) (see Scheme 1). Case **a** is that of the oligomers and polymers described by Osuka^[8] of Zn porphyrins that are σ -bonded through the *meso*-position and case **b** of the structures obtained by self-assembly of the diprotonated 4'-sulfonatophenyl- or phenyl-substituted 5,10,15,20-tetraarylporphyrins (H_2TPPS_4 , H_2TPPS_3 , H_2TPPS_{2a} , H_2TPPS_{2o} , and H_2TPPS_1).^[8]

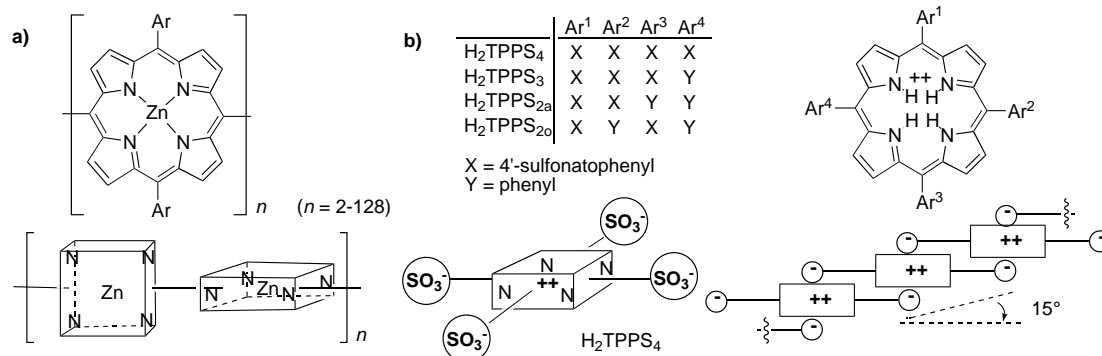
Case a: meso-coupled 5,15-diaryl-substituted porphyrins:^[8]

These π chromophore systems, in spite of being separated by only one C–C σ bond, should be considered as ring-localized π chromophores owing to the 90° dihedral angle between rings. The absorption spectra of these compounds show a split of the B-band in two bands of approximately the same oscillator strength; one is red-shifted and the other does not show change of energy in respect to the monomeric porphyrin. The D_{2d} (highest possible symmetry) arrangement of the transition dipole moments (see Figure 3) explains the observed split, composed of the non-shifted B_y transition and the red-shifted B_x transition.^[8d] The arrangement corresponding to two individual porphyrins C_2 (Gouterman's model) would result in one red-shifted degenerate band. Further, for the homologous series of these compounds it has been shown that the red-shift value depends on the number of coupled porphyrin units,^[8c] in agreement with that expected for a one-dimensional extended exciton coupling ($\Delta E = \Delta E_o \cos[\pi/(n + 1)]$).^[10]

In conclusion, the experimental results can be explained by using pairs of dipole transition moments arranged according to the highest possible symmetry in agreement with the molecular geometry and an extended exciton coupling.

Case b: homoassociates of diprotonated 4'-sulfonatophenyl meso-substituted porphyrins:^[9]

The homoassociates of case **b** give colloidal solutions of mesoscopic structures^[12] based on intermolecular-stabilized zwitterions. These solutions by evaporation give a condensed phase that has been identified as a lyotropic liquid crystal.^[9c] The solution homoassociates are J-aggregates of ribbon-like stepped, stacked porphyrins (red shifted B- and Q-bands; $\Delta E_B \approx 2500 \text{ cm}^{-1}$, $\Delta E_Q \approx 1350 \text{ cm}^{-1}$). These J-aggregates give H-aggregation (blue-



Scheme 1.

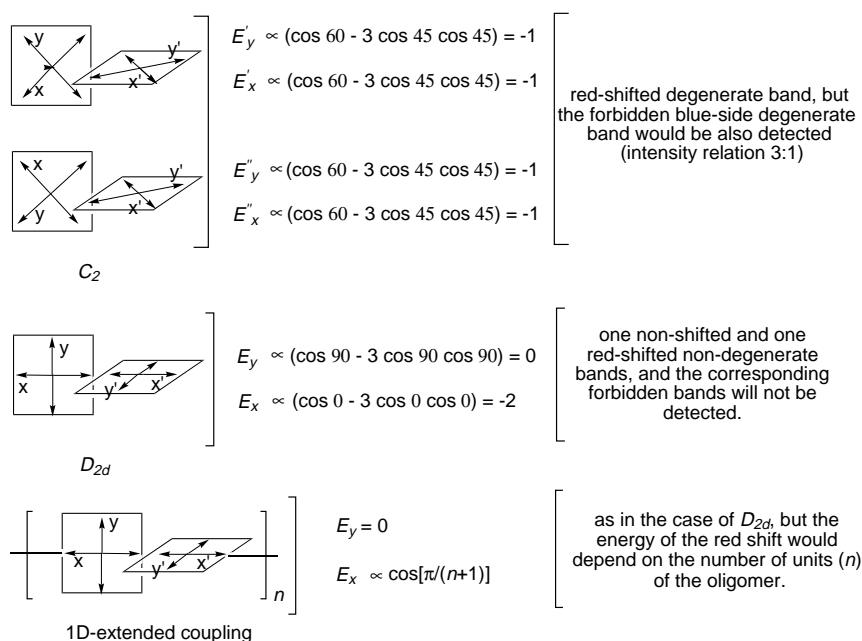


Figure 3. Expected B-bands for the exciton coupling in a porphyrin dimer side-to-side and 90° diedral angle between both porphyrin planes for several transition dipole moment arrangements. Only the D_{2d} arrangement explains the experimental results of case a,^[8] which also shows a one-dimensional extended exciton coupling, that is, energy shift depending on the number of coupled chromophores.

shifted B-band; $\Delta E \approx 850 \text{ cm}^{-1}$; Q-bands overlapped by those of the J-aggregate). The blue- and red-shifted absorptions correspond to independent perturbations near to the extreme points showed in Figure 1, that is, when the allowed state is the high- or low-energy state (H- and J-aggregation, respectively) rather than the blue or red site of an exciton-coupling perturbation with intermediate θ values (Scheme 1). All this has been inferred from the following results.

In the formation of these colloidal solutions spontaneous chiral symmetry breaking occurs, which is detected through their circular dichroism (CD) spectra.^[9d] These spectra show bisignate CD signals for the B-bands of the H- and the J-aggregation; this indicates that both transitions are degenerate. Chirality is due to the folding of the H- and J-aggregation (Figure 4), and the results point to the presence of two orthogonal chirality axes corresponding to the J and the H-aggregation.

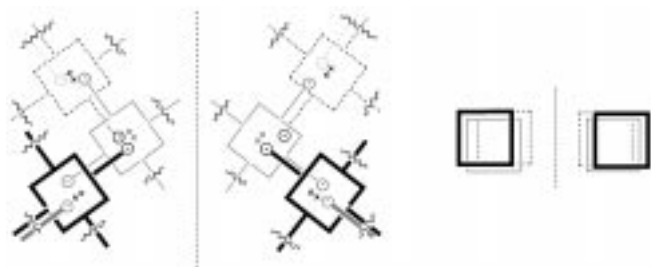


Figure 4. Chirality originated by folding in the J- and H-aggregates of case b.

For the J-aggregation, 180° and 90° arrangements (in Scheme 1 only the 180° arrangement is illustrated) show

similar UV/Vis absorptions, as inferred from i) the study of the homoassociation of the homologous series of 4'-sulfo-nato-substituted tetraphenylporphyrins^[9b] and ii) the chirality of the J-aggregates.^[9d]

i) The homoassociates of the homologous series show similar absorption spectra in spite of the fact that some terms should give 90° arrangements (e.g., $\text{H}_2\text{TPPS}_{2a}$).

ii) The UV/Vis spectra do not change significantly when the intensity of the CD signals increase, that is when folding increases.

The application of the exciton coupling model shows that the degeneracy of the homo-associate absorption bands can only be explained by assuming transition dipole moments ac-

ording to Gouterman's model (see Figure 5 for the simple dimer model).^[9d]

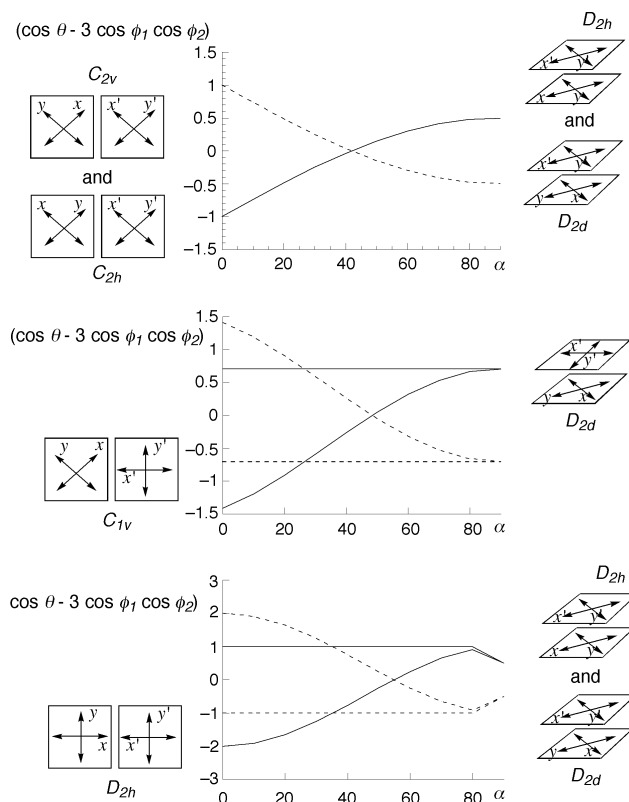


Figure 5. Expected B-bands for the exciton coupling in a porphyrin dimer with parallel porphyrin planes and at several angles (α); from $\alpha = 0^\circ$ (side-to-side; J-aggregation) to $\alpha = 90^\circ$ (face-to-face; H-aggregation) structures. Only the C_{2v} - C_{2h} arrangement (transition dipole moments according Gouterman^[6]) explains the experimental spectra of case b.^[9]

An interesting characteristic of the absorption spectra of these homoassociates, and in contrast with the case **a**, is that at any level of association, that is, from very short to long chain lengths, the homoassociated absorption bands appear at the same wavelength; this suggests a non-extended exciton coupling. As non-extended exciton coupling we understand the case in which each chromophore interaction depends on R^{-3} . Such a non-extended exciton coupling explains the similar absorption spectra for the achiral 180° and the chiral 90° arrangements. The interaction energy, which depends on R^{-3} , for the 1–2 interaction ($R_{12} \approx 10 \text{ \AA}$) would be eight times higher than the 1–3 interaction ($R_{13} \approx 20 \text{ \AA}$), and two orders of magnitude higher than the 1–4 interaction. In consequence a non-extended coupling can be approximated to a porphyrin chromophore perturbed by two neighboring rings (a trimer model). The corner ring in the 90° fold would show the same exciton coupling interactions as in the case of the 180° arrangement. The neighboring rings to a corner ring would show the same 1–2 interactions as for the linear arrangement, but different 1–3 interactions. These last interactions would result in only a slight split of the degenerate B_J -band, which, depending on the ratio of foldings, would be detected through a broadening of the absorption band. This broadening of the band has been experimentally detected for the compounds of the series that should result in a significant amount of 90° arrangements, for example H_2TPPS_{2A} .^[9b,d] This broadening is in contrast with the characteristic Lorenz pattern of the J-aggregates.

In conclusion, the experimental results can be explained using a non-extended exciton coupling and non-modified dipole transition moments in respect to the monomeric porphyrin.

Ionic versus covalent bonding: Cases **a** and **b** show the different effects exerted through an ionic or a covalent bond between the organic residues of a supramolecular structure. An ionic bond forms a Coulomb barrier between the electron systems of the interacting chromophores, which in spite of the mutual perturbation the electron configuration of the excited states is not affected (case **b**). In case **a**, in spite of having localized π chromophores due to the orthogonality between chromophores, the *meso* C–C σ bond implies that the electronic configuration of the excited states is determined by all electrons of the molecular entity. This can be detected through the relative orientation of the transition dipole moments of the two chromophores. In fact, this is an example of what is known by organic chemists as π^* contamination.

Notice that supramolecular metalloporphyrin structures in which a peripheral covalent bonded group acts as intermolecular ligand on the metal atom (e.g., ref. [7b]) have UV/Vis spectra that are also explained by using the exciton coupling model, as for case **a**.^[12] In that case, as expected, the ligand–metal interaction should be considered to play a similar role to the covalent bond, that is, all electrons of the system contribute the electronic configuration of the excited states.

Solid-state excitons and their relation to the molecular models used in the description of organic molecules: The cases described here are examples of the description at molecular

level (orbital model) of the excitons as described in solid-state physics (band model).^[13]

Case **a** would correspond to the transcription at molecular level of a Wannier–Mott exciton, that is, in which the distance between electron and hole can be greater than the lattice constant (porphyrin chromophore unit).^[14] This can only occur if there is a band structure between units (valence band \leftrightarrow HOMO; conducting band \leftrightarrow LUMO) and when in the electron–hole interaction the exchange energy is a more important contribution than the coulombic energy. In this respect, the comparison of the homologous series by steady-state fluorescence spectra^[8c] points to coherence lengths of 6–8 porphyrin units, that is, also in agreement with the simple model for one-dimensional extended exciton coupling, when $\cos[\pi/(n+1)]$ approaches a value of 1.^[10]

Case **b** corresponds to a monodimensional Frenkel exciton, which in solid phases is typical for strongly ionic-bound materials. This has already been proposed for the J-aggregates of other systems^[15] and also experimentally detected for the case **b**.^[16] Here the exciton is placed in the same unit cell, but the electron and the hole propagate together to other unit cells. Note, that the size of this Frenkel exciton, being larger the lattice constant (one porphyrin unit), must be larger than the typical ones for inorganic semiconductors ($\approx 5 \text{ \AA}$).^[1]

In this context, the study of the electronic spectra of these porphyrin systems could assist to the prediction of the exciton type. For example, in the case **b** the steady-fluorescence spectra shows the presence of two different exciton couplings, that is, in the H- and in the J-aggregation axis.^[17] The mesoscopic solutions of the homoassociates show different fluorescence spectra from their monomers (monomer $\lambda_{em} \approx 670\text{--}675 \text{ nm}$; homoassociate $\lambda_{em} \approx 715\text{--}725 \text{ nm}$), and the excitation spectrum, measured at the $S_1 \rightarrow S_0$ transition of the homoassociate, correlates well with the absorption bands corresponding to the J-aggregation, without the contribution of the B_H absorption. In fact, the point-dipole approximation of exciton coupling already predicts that no fluorescence spectra will be detected for the case of H-aggregation.^[2] These experimental results suggest that two different Frenkel excitons, each of them in the structural axis that defines the H- and J-aggregation, should be detected.

We believe that many research objectives are being raised in this topic. For example, questions are open referring the intermediate cases of excitons, the exciton trapping and self-trapping, and, with the goal of applications, the design of organic materials with high exciton densities.^[1]

Acknowledgement

The financial support from the Ministerio de Ciencia y Tecnología (Grants PB98-1240-C02-01 and AGL2000-0975) is gratefully acknowledged.

- [1] M. Pope, C. E. Swenberg, *Electronic Processes in Organic Crystals and Polymers*, Oxford University Press, New York, 1999.
- [2] M. Kasha, H. R. Rawls, M. A. El-Bayoumi, *Pure Appl. Chem.* **1965**, *11*, 371–392.
- [3] a) N. Harada, K. Nakanishi, *Circular Dichroic Spectroscopy. Exciton Coupling in Organic Stereochemistry*, University Science Books, Mill

- Valley, CA, **1983**; b) D. A. Lightner, J. K. Gawronski, W. M. D. Wijekoon, *J. Am. Chem. Soc.* **1987**, *109*, 6354–6362.
- [4] E. E. Jelly, *Nature* **1936**, *138*, 1009; b) G. Scheibe, *Angew. Chem.* **1936**, *49*, 563.
- [5] See, for example: a) D. C. Barber, R. A. Freitag-Beeston, D. G. Whitten, *J. Phys. Chem.* **1991**, *95*, 4074–4086; b) H. Eichhorn, D. Woehrlé, D. Pressner, *Liq. Cryst.* **1997**, *22*, 643–653.
- [6] a) M. Gouterman, *J. Mol. Spectrosc.* **1961**, *6*, 138–163; b) M. Gouterman, *The Porphyrins, Vol. III*, Academic Press, London, **1978**, pp. 1–165.
- [7] See, for example: a) J.-H. Fuhrhop, C. Demoulin, C. Boettcher, J. Köning, U. Siggel, *J. Am. Chem. Soc.* **1992**, *114*, 4159–4165; b) Y. Kobuke, H. Miyaji, *J. Am. Chem. Soc.* **1994**, *116*, 4111–4112; c) M. C. Endisch, J. H. Fuhrhop, J. Buschmann, P. Luger, U. Siggel, *J. Am. Chem. Soc.* **1996**, *118*, 6671–6680; d) J. M. Kroon, R. B. M. Koehorst, M. Dijk, G. M. Sanders, E. J. R. Sudhölter, *J. Mater. Chem.* **1997**, *7*, 615–624; e) N. C. Maiti, S. Mazumdar, X. Peryasamy *J. Phys. Chem.* **1998**, *102*, 1528–1538; f) V. V. Borokov, J. M. Lintuluoto, M. Fujiki, Y. Inoue *J. Am. Chem. Soc.* **2000**, *122*, 4403–4407; g) G. A. Schick, I. C. Schreiman, R. W. Wagner, J. S. Lindsey, D. F. Bocian, *J. Am. Chem. Soc.* **1986**, *111*, 1344–1350; h) A. Osuka, K. Maruyama, *J. Am. Chem. Soc.* **1988**, *110*, 4454–4456; i) A. P. H. J. Schenning, F. B. G. Benneker, H. P. M. Geurts, X. L. Liu, R. J. M. Nolte, *J. Am. Chem. Soc.* **1996**, *118*, 8549–8552; j) J. H. van Esch, A.-M. P. Peters, R. J. M. Nolte, *Chem. Commun.* **1990**, 638–639.
- [8] a) A. Osuka, K. Maruyama, *J. Am. Chem. Soc.* **1988**, *110*, 4454–4456; b) T. Nagata, A. Osuka, K. Maruyama, *J. Am. Chem. Soc.* **1990**, *112*, 3054–3059; c) N. Aratani, A. Osuka, Y. H. Kim, D. H. Jeong, D. Kim, *Angew. Chem.* **2000**, *112*, 1498–1251; *Angew. Chem. Int. Ed.* **2000**, *39*, 1458–1462; added in proof: d) Y. H. Kim, D. H. Jeong, H. S. Cho, S. K. Kim, N. Arataani, A. Osuka *J. Am. Chem. Soc.* **2001**, *123*, 76–86.
- [9] a) J. M. Ribó, J. Crusats, J.-A. Farrera, M. L. Valero, *Chem. Commun.* **1994**, 681–682; b) R. Rubires, J. Crusats, Z. El-Hachemi, T. Jaramillo, M. López, E. Valls, J.-A. Farrera, J. M. Ribó, *New J. Chem.* **1999**, 189–198; c) J. M. Ribó, R. Rubires, Z. El-Hachemi, J.-A. Farrera, L. Campos, G. L. Pakhomov, M. Vendrell, *Mater. Sci. Eng. C* **2000**, *11*, 107–115; d) R. Rubires, J.-A. Farrera, J. M. Ribó, *Chem. Eur. J.* **2001**, *7*, 436–446.
- [10] a) V. Czikkely, H. D. Forsterling, H. Kuhn, *Chem. Phys. Lett.* **1970**, *6*, 207–210; b) P. W. Bohn, *Ann. Rev. Phys. Chem.* **1993**, *4*, 37–60.
- [11] N. Micali, F. Mallamace, A. Romeo, R. Purrello, L. Monsú Scolaro, *J. Phys. Chem. B* **2000**, *104*, 5897–5904.
- [12] The UV/Vis spectrum of the dimer of ref. [7b] can be explained by the case D_{2h} (Figure 4) for an angle $\alpha \approx 40^\circ$.
- [13] V. G. Lyssenko in *Encyclopedia of Materials Science and Engineering, Vol. 2* (Ed.: M. B. Bever), Pergamon, Oxford, UK and MIT Press, Cambridge, MA, **1986**, pp. 1585–1589.
- [14] Note added in proof: Wannier–Mott excitons have been assigned to a similar system to that of case **a**, on the basis of polarizability measurements of the photoexcited states: J. J. Piet, P. N. Taylor, B. R. Wegewijs, H. L. Anderson, A. Osuka, J. Warman, *J. Chem. Phys. B* **2001**, *105*, 97–104.
- [15] P. O. J. Scherer, S. F. Fischer, *Chem. Phys.* **1984**, *86*, 269–283.
- [16] a) K. Misawa, T. Kobayashi, *J. Chem. Phys.* **1999**, *110*, 5844–5850; Added in proof: c) H. Kano, T. Saito, T. Kobayashi, *J. Phys. Chem. B* **2001**, *105*, 413–419.
- [17] R. Rubires, Ph.D. Thesis, University of Barcelona (Spain), **2000**.